

The gravitational wave echoes from the black hole with three-form fields

Natthason Autthisin,^{1,*} Supakchai Ponglertsakul,^{2,†} and Daris Samart^{1,‡}

¹*Khon Kaen Particle Physics and Cosmology Theory Group (KKPaCT),*

Department of Physics, Faculty of Science,

Khon Kaen University, Khon Kaen, 40002, Thailand

²*Strong Gravity Group, Department of Physics, Faculty of Science,*

Silpakorn University, Nakhon Pathom 73000, Thailand

Abstract

In this work, we study of massless three-form black hole, where the three-form fields are higher p -form gauge fields with $p = 3$. These give rise to the Schwarzschild-de Sitter (Sch-dS)-like solution through an effective cosmological constant represented by a_1 . We analyze this solution under gravitational perturbations and find that it exhibits a single-peak potential. For this case, no echoes are produced. Furthermore, we consider the massive case of the three-form fields by introducing a Stueckelberg field to restore gauge invariance and to investigate its effect on GWs at late times. In this case, the potential exhibits a double-peak structure, with the modified potential appearing beside the gravitational perturbation potential. We also examine the impact of the relevant parameters as well as the influence of the parameter c_0 , which arises from the equation of motion of the Stueckelberg field. For a large value of a_1 , the two peaks of the potentials are close together, while c_0 affects the amplitude and decay rate of the time-domain waveform, resulting in no echoes. For small values of a_1 , the peaks of the potentials are widely separated and c_0 influences both the phase and the amplitude of the echoes. In addition, the quasinormal frequencies of the black hole are also calculated using both the WKB and Prony methods. As results, these provide a potential avenue for testing deviations from GR and probing possible signatures of quantum gravity through future GWs observations.

*Electronic address: natthasorn_ut@kkumail.com

†Electronic address: supakchai.p@gmail.com

‡Electronic address: darisa@kku.ac.th

I. INTRODUCTION

The modification of gravitational theory and the empirical testing of the predictions derived from GR constitute essential areas of research in the fields of theoretical physics and astrophysics. One of the most fascinating predictions of GR is the existence of GWs. In 2016, LIGO successfully detects gravitational waves from a binary black hole merger [1]. It has opened a new era in black hole physics and the testing of theories of gravity in the strong-field regime. Recently, NANOGrav detected the existence of a stochastic gravitational wave background from pulsar timing array (PTA) observations in the nanohertz band [2]. This discovery has a significant impact on the field of gravitational wave astronomy and significantly improves observational techniques.

In general, gravitational waves can be regarded as a perturbation of the gravitational field. The study of perturbation around black holes is firstly pioneered by Regge and Wheeler in 1957 [3] where they consider gravitational perturbation around Schwarzschild black hole. Their result is later extended to electrically charged Reissner-Nordström black hole [4] and Kerr black hole [5, 6] for gravitational and electromagnetic perturbations. Another prominent result from the study of black hole perturbation is discovered by Vishveshwara in 1970 [7]. He studies evolution of gravitational wave package around fixed Schwarzschild space-time. It is found that the late time signal is dominated by damping oscillation frequency. Moreover, the oscillation and damping frequencies are solely characterized by one black hole parameter i.e., black hole's mass in case of the Schwarzschild black hole (Sch-BH). These oscillations are known as QNMs and corresponding frequencies are quasinormal frequencies. It is expected that a late time signal of GWs from a binary black hole merger must be dominated by damped oscillation or a ringdown phase. At late time, a gravitational perturbation can be treated at a linearized level and therefore the oscillation modes will be described by the QNMs. For this reason, the study of QNMs has attracted significant attentions and become a very crucial tool to explore physical properties of black holes [8], hairy black holes [9–11] and compact objects [12–17]. Additionally, several works have been devoted to extracting QNMs signal from the gravitational waves [18–21]. In 2000, Ferrari and Kokkotas [22] extend the calculation of the time-domain perturbation equation of relativistic stars and find the emergence of series of late-time signals after the ringdown phase. This series of late-time signals is called gravitational wave echoes. Gravitational wave echoes are ex-

pected to be detected in the future [23, 24]. Theoretically, the existence of gravitational wave echoes arises from the presence of double-peaked effective potentials. The bouncing of perturbations between the double-peaked effective potentials causes the echoes to occur. Various ECOs models, particularly black holes and wormholes, have been shown to manifest double-peaked potentials and generate echoes in Refs.[24–32]. For perturbations, some ECOs models naturally yield a potential with two peaks. In other cases, such as massive gravity black holes in massive gravity [28], the Stueckelberg field is employed to modify the potential to create a double-peaked structure.

At present, there is ongoing development and a search for black hole models that are consistent with observational results. In cosmology, many cosmological problems can be described by scalar fields. In the context of ECOs, there are many models represented by scalar fields. In string theory, there exists three-form fields that have the same degrees of freedom as a scalar field [33, 34]. Three-form fields can be used to describe inflation, structure formation, and may also serve as a candidate for dark energy in explaining the expansion of the universe [35–40]. Screening solutions involving three-form fields that are conformally coupled to matter have also been examined in [41]. Moreover, three-form fields have been used to study black hole and wormhole [42–45]. This work study gravitational perturbation of black hole supported by three-form fields. The solution for a black hole with a three-form fields have already been found in [43]. It was shown that the solution has the Sch-dS-like form. It includes the existence of an effective cosmological constant, which is advantageous for exploring the expanding universe.

Typically, perturbations in de Sitter spacetime have a single-peak potential and do not produce echoes [46, 47]. In this work, we introduce a Stueckelberg field, inspired by the massive three-form fields case, to add an extra contribution to the effective potential and generate a double-peak structure. We use the similar manner as done in Ref.[28] to obtain gravitational wave echoes. Furthermore, we investigate how the amplitude of both peaks influence the echoes.

The paper is organized as follows. In section II, we review general formalism of three-form fields in Einstein gravity. In section III, based on a static and spherically symmetric background, we first derive the gravitational field equations and then obtain the black hole solution for zero potential. The gravitational perturbation, time-domain wave equation, method for calculating QNMs and modification of the effective potential will be discussed in

section IV. Then, in section V, we show numerical calculations of both single and double-peak potentials, time-domain strain, and QNMs of the three-form black hole for both massless and massive cases. Finally, we summarize our key results in section VI.

II. THE THREE-FORM FIELD : GENERAL FORMALISM

In this section, we provide a brief review of the three-form fields. The action for Einstein gravity coupled to a standard three-form fields are given by [43]

$$S = \int d^4x \sqrt{-g} \left[\frac{1}{2\kappa^2} R - \frac{1}{48} F_{\mu\nu\rho\sigma} F^{\mu\nu\rho\sigma} - V(A^2) \right], \quad (1)$$

where $g = \det g_{\mu\nu}$, $\kappa^2 \equiv 8\pi G$, $A^2 = A_{\mu\nu\rho} A^{\mu\nu\rho}$ and R is a Ricci scalar. Additionally, $F_{\mu\nu\rho\sigma}$ is a field strength tensor of the three-form fields, $A_{\mu\nu\rho}$. It is defined as

$$F_{\mu\nu\rho\sigma} = \nabla_\mu A_{\nu\rho\sigma} - \nabla_\nu A_{\mu\rho\sigma} + \nabla_\rho A_{\sigma\mu\nu} - \nabla_\sigma A_{\rho\mu\nu}. \quad (2)$$

In addition, $V(A)$ is the potential of the three-form fields. Varying the action in (1) with respect to $g^{\mu\nu}$, the Einstein field equation (EFE) is given by

$$G_{\mu\nu} = \kappa^2 T_{\mu\nu}, \quad (3)$$

where $G_{\mu\nu} \equiv R_{\mu\nu} - \frac{1}{2} g_{\mu\nu} R$. The energy-momentum tensor of the three-form fields reads

$$T_{\mu\nu} \equiv \frac{1}{6} F_{\mu}{}^{\rho\sigma\tau} F_{\nu\rho\sigma\tau} + 6 \frac{\partial V(A^2)}{\partial(A^2)} A_{\mu}{}^{\rho\sigma} A_{\nu\rho\sigma} + g_{\mu\nu} \left[\frac{1}{48} F_{\alpha\beta\rho\sigma} F^{\alpha\beta\rho\sigma} - V(A^2) \right]. \quad (4)$$

The equation of motion of the three-form is obtained by varying with respect to the $A_{\mu\nu\rho}$. One finds

$$\nabla_\sigma F^{\sigma\mu\nu\rho} - 12 \frac{\partial V(A^2)}{\partial(A^2)} A^{\mu\nu\rho} = 0. \quad (5)$$

The three-form gauge field can be represented as a product of the one-form dual vector and Levi-Civita tensor

$$A_{\mu\nu\rho} = \sqrt{-g} \epsilon_{\mu\nu\rho\sigma} B^\sigma, \quad (6)$$

where the B^σ is the one-form dual vector of the three-form fields, $A_{\mu\nu\rho}$. The one-form dual vector can be written using the radial ansatz [43]

$$B^\sigma = (0, \zeta(r), 0, 0)^\top, \quad (7)$$

where $\zeta(r)$ is a generic parametrization of the three-form fields. The three-form field function ζ will be determined from the EFE (3) and equation of motion (5).

With the ansatz (7), the kinetic term of the three-form field may be expressed explicitly as

$$-\frac{1}{48}F^2 = -\frac{1}{48}F_{0123}F^{0123} = \frac{1}{2}(\nabla_\mu B^\mu)^2. \quad (8)$$

In the following section, we shall consider static spherically symmetric solution of Einstein-three-form field theory.

III. BLACK HOLE WITH THREE-FORM FIELDS

In this section, we calculate the EFE from the three-form field and obtain the black hole solution supported by the three-form field.

A. Black hole metric and field equations

In this work, we examine the following static and spherically symmetric ansatz

$$ds^2 = -e^{\alpha(r)}dt^2 + e^{\beta(r)}dr^2 + r^2d\Omega^2, \quad (9)$$

where $d\Omega^2 = d\theta^2 + \sin^2\theta d\phi^2$. On this background geometry, the invariant A^2 is given by

$$A^2 = -6e^{\beta(r)}\zeta(r)^2, \quad (10)$$

and the term expressing the kinetic energy of the three-form is provided explicitly by

$$F^2 = -6\left[\zeta\left(\alpha' + \beta' + \frac{4}{r}\right) + 2\zeta'\right]^2, \quad (11)$$

where a prime denotes the derivative with respect to the radial coordinate. EFE (5) can now be written in terms of ζ , as

$$2\zeta'' + \left(\alpha' + \beta' + \frac{4}{r}\right)\zeta' + \left(\alpha'' + \beta'' - \frac{4}{r^2}\right)\zeta + 2\frac{\partial V}{\partial \zeta} = 0. \quad (12)$$

From the energy-momentum tensor (4) and the metric ansatz (9), we obtain the components of energy-momentum tensor of the three-form fields as

$$T_t^t = -\rho = \frac{F^2}{48} - V + \frac{\partial V}{\partial \zeta}, \quad (13)$$

$$T_r^r = p_r = \frac{F^2}{48} - V, \quad (14)$$

$$T_\theta^\theta = T_\phi^\phi = p_t = T_t^t. \quad (15)$$

We identify ρ , p_r and p_t with the energy density, the radial pressure, and the tangential pressure, respectively, in term of the three-form. We notice that $\rho = -p_t$. Now by setting $\kappa = 1$ for simplicity, three components of EFE (3) read

$$\frac{e^{-\beta}}{r^2} (1 - r\beta' - e^\beta) = \frac{F^2}{48} - V + \frac{\partial V}{\partial \zeta}, \quad (16)$$

$$\frac{e^{-\beta}}{r^2} (1 + r\alpha' - e^\beta) = \frac{F^2}{48} - V, \quad (17)$$

$$\frac{e^{-\beta}}{2} \left[\alpha'' + \left(\frac{1}{r} + \frac{\alpha'}{2} \right) (\alpha' - \beta') \right] = \frac{F^2}{48} - V + \frac{\partial V}{\partial \zeta}. \quad (18)$$

Combining (16) and (17), we find

$$\alpha' + \beta' = -re^\beta \zeta \frac{\partial V}{\partial \zeta}. \quad (19)$$

By considering (16) and (18), we obtain

$$\frac{2}{r^2} (1 - r\beta' - e^\beta) = \alpha'' + \left(\frac{1}{r} + \frac{\alpha'}{2} \right) (\alpha' - \beta'). \quad (20)$$

With a given potential V , there are three coupled differential equations (12),(19)–(20) for three undetermined functions $\alpha(r)$, $\beta(r)$ and $\zeta(r)$. In the next subsection, we will solve this equation system for the black hole solution.

B. Black hole solution with three-form fields

To obtain a static spherically symmetric black hole solution, we shall set the three-form field's potential $V = 0$. This is effectively equivalent to the massless three-form fields. Thus from (19), we get

$$\alpha = -\beta, \quad (21)$$

This greatly simplified our set of equations. Hence, (20) becomes

$$\alpha'' + \alpha'^2 = \frac{2}{r^2} (1 - e^{-\alpha(r)}) . \quad (22)$$

This equation can be solved by setting $\alpha = \ln f$. Thus, we obtain the solution

$$f(r) = 1 + \frac{c_1}{r} + c_2 r^2, \quad (23)$$

where c_1 and c_2 are the constants of integration. The parameter c_1 can be determined by comparing it with the Schwarzschild solution, i.e., $c_1 = -2M$, where M is the mass of the black hole. To determine c_2 , we consider the following. By using, (21), the equation of motion of the three-form fields (12) can be re-casted into

$$\zeta'' + \frac{2}{r}\zeta' - \frac{2}{r^2}\zeta = 0, \quad (24)$$

which yields the following solution

$$\zeta(r) = a_1 r + \frac{a_2}{r^2} \quad (25)$$

where a_1 and a_2 are arbitrary constants of integration. Therefore, the kinetic term of the three-form field can be written explicitly in terms of constant a_1

$$F^2 = -216a_1^2. \quad (26)$$

the constant c_2 can be written in terms of a_1 by putting the exact form of $f(r)$ into (18). As a result, we obtain $c_2 = -3a_1^2/2$. Therefore, we can express $f(r)$ in an Sch-dS-like solution. It reads

$$e^\alpha = e^{-\beta} = f(r) = 1 - \frac{2M}{r} - \frac{3}{2}a_1^2 r^2, \quad (27)$$

where a_1 can be related to an effective cosmological constant (Λ_{eff}) emerging from the three-form field via $\Lambda_{\text{eff}} \equiv 9a_1^2/2$. We can rewrite the metric (9) as

$$ds^2 = - \left(1 - \frac{2M}{r} - \frac{3}{2}a_1^2 r^2 \right) dt^2 + \left(1 - \frac{2M}{r} - \frac{3}{2}a_1^2 r^2 \right)^{-1} dr^2 + r^2 d\Omega^2. \quad (28)$$

The Sch-dS spacetime has two horizons: the black hole horizon is at $r = r_h$, and the cosmological horizon is at $r = r_c$, where $r_c > r_h$. The function f vanishes at r_h, r_c , and $r_0 = -(r_h + r_c)$. The function f can be expressed as

$$f(r) = \frac{3a_1^2}{2r}(r - r_h)(r_c - r)(r - r_0). \quad (29)$$

The root of cubic equations can be expressed in analytic form as follows

$$r_h = \frac{2\sqrt{2}}{3a_1} \cos \left(\frac{1}{3} \arccos \left(-\frac{9Ma_1}{\sqrt{2}} \right) + 4\pi \right), \quad (30)$$

$$r_c = \frac{2\sqrt{2}}{3a_1} \cos \left(\frac{1}{3} \arccos \left(-\frac{9Ma_1}{\sqrt{2}} \right) \right), \quad (31)$$

$$r_0 = \frac{2\sqrt{2}}{3a_1} \cos \left(\frac{1}{3} \arccos \left(-\frac{9Ma_1}{\sqrt{2}} \right) + 2\pi \right). \quad (32)$$

In this work, we consider the value of a_1 from the near-extremal case to the case where the black hole horizon r_h and the cosmological horizon r_c are widely separated, as shown in Fig. 1. Specifically, the value of a_1 starts from 0.3 and is successively halved down to 0.0046875, as shown by the red to green lines in Fig. 1.

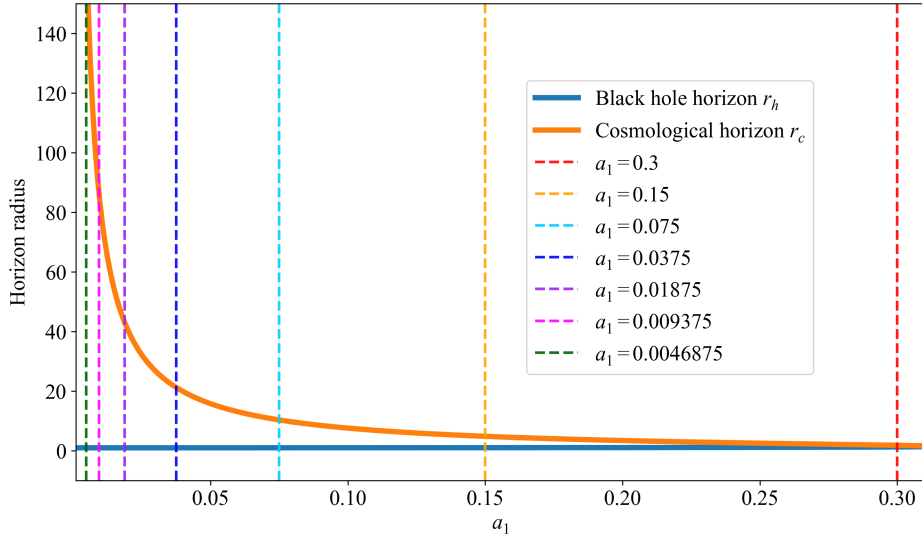


FIG. 1: Horizon radius as functions of the parameter a_1 , with $M = 1/2$. The blue and orange curves represent the black hole horizon radius r_h and the cosmological horizon radius r_c , respectively. Vertical dashed lines indicate specific values of a_1 used in the analysis throughout this work.

We also introduce the surface gravity k_i associated with the horizon $r = r_i$, as defined by the relation $k_i = \frac{1}{2} |df/dr|_{r=r_i}$. Then, we have

$$k_h = \frac{3a_1^2(r_c - r_h)(r_h - r_0)}{4r_h}, \quad (33)$$

$$k_c = \frac{3a_1^2(r_0 - r_c)(r_c - r_h)}{4r_c}, \quad (34)$$

$$k_0 = \frac{3a_1^2(r_c - r_0)(r_0 - r_h)}{4r_0}. \quad (35)$$

We define the tortoise coordinate $r_* = \int f^{-1} dr$. From the surface gravity k_i , we can express f^{-1} as

$$f^{-1} = \frac{1}{2k_h(r-r_h)} + \frac{1}{2k_c(r_c-r)} + \frac{1}{2k_0(r-r_0)}. \quad (36)$$

Therefore, the tortoise coordinate r_* in Sch-dS spacetime can be obtained exactly [48]

$$r_* = \frac{1}{2k_h} \ln \left(\frac{r}{r_h} - 1 \right) - \frac{1}{2k_c} \ln \left(1 - \frac{r}{r_c} \right) + \frac{1}{2k_0} \ln \left(1 - \frac{r}{r_0} \right). \quad (37)$$

In the next section, we will explore gravitational perturbation in black hole spacetime.

IV. GRAVITATIONAL PERTURBATION

In the previous section, we obtain the three-form black hole solution. In this section, we study perturbations in the black hole spacetime. The type of perturbation examined in this work is a gravitational perturbation. We analyze the behavior of effective potentials and introduce an additional term into the potential. This additional term will play the role as a mass and an interaction term for the three-form fields. We also examine the time-domain profiles of gravitational perturbation around three-form black holes. In addition, we also determine the QNMs of the three-form black hole.

We start by considering the following linear perturbation on the spacetime metric

$$g_{\mu\nu} = g_{\mu\nu}^0 + h_{\mu\nu}. \quad (38)$$

where $g_{\mu\nu}^0$ is background metric (28). The small perturbation is denoted by rank-2 tensor $h_{\mu\nu}$. From [3, 49], the canonical form of $h_{\mu\nu}$ for the gravitational perturbations in the Regge-Wheeler gauge is given by

$$h_{\mu\nu} = \begin{bmatrix} 0 & 0 & 0 & h_0(t, r) \\ 0 & 0 & 0 & h_1(t, r) \\ 0 & 0 & 0 & 0 \\ h_0(t, r) & h_1(t, r) & 0 & 0 \end{bmatrix} \sin \theta \left(\frac{\partial}{\partial \theta} \right) P_l(\cos \theta), \quad (39)$$

where $P_l(\cos \theta)$ is the Legendre polynomial of order l with two unknown functions $h_0(t, r)$ and $h_1(t, r)$.

A. Time-domain : wave-like equation

To obtain the Schrödinger-like equation for the gravitation perturbation, we define time-domain wavefunction as expressed below

$$\Psi(t, r) = f(r) \frac{h_1(t, r)}{r}, \quad (40)$$

Having use the standard linearization of EFE with Eqs.(39) and (40), one finds the Schrödinger-like equation as

$$\left(\frac{\partial^2}{\partial t^2} - \frac{\partial^2}{\partial r_*^2} + V_{\text{GP}}(r) \right) \Psi(t, r_*) = 0, \quad (41)$$

where we define the effective potential from gravitational perturbation V_{GP} as

$$V_{\text{GP}}(r) = f(r) \left(\frac{l(l+1)}{r^2} - r \frac{d}{dr} \left(\frac{f(r)}{r^2} \right) - \frac{2}{r^2} \right). \quad (42)$$

We note that the $h_0(t, r)$ can be eliminated via the linearized EFE.

1. The modified potential from massive three-form fields

In the previous section, black hole solution with massless three-form fields is obtained. However, one can investigate how massive three-form fields affects to gravitational waves. In this section, we examine the effect of massive three-form fields to gravitational waves. We are interested in how the energy-momentum tensor of mass term modifies the axial perturbation potential to produce a double-peak structure of the effective potential. From previous work in [28] and standard gravitational perturbation analysis, the gravitational perturbation equation receives additional potential terms if the background matter fields couple to the metric in a non-trivial radial profile.

We start by considering the action of a massive three-form, which can be written as

$$S = \int d^4x \sqrt{-g} \left(\frac{1}{2\kappa^2} R - \frac{1}{48} F_{\mu\nu\rho\sigma} F^{\mu\nu\rho\sigma} - \frac{1}{2} m_A^2 A_{\mu\nu\rho} A^{\mu\nu\rho} \right), \quad (43)$$

where $m_A \ll 1$ is the small mass of three-form fields. According to the one-form dual vector of the three-form in Eq.(6) and Eq.(8), the action become massive spin-1 field as

$$S = \int d^4x \sqrt{-g} \left(\frac{1}{2\kappa^2} R + \frac{1}{2} (\nabla_\mu B^\mu)^2 - \frac{1}{2} m_A^2 B^\mu B_\mu \right). \quad (44)$$

In contrast to the scalar perturbation where scalar field's mass can be introduced directly into the Lagrangian, adding mass term to vector field will break gauge invariance. In addition, the mass term leads to pathological problems such as ghost and unstable longitudinal modes [50–52].

Similarly, the first massive graviton theory introduced by Fierz and Pauli [53] is known to suffer from the van Dam-VeltmanZakharov (vDVZ) discontinuity [54, 55] where GR is not recovered in the massless graviton limit and the Boulware-Deser ghost [56] which leads to additional unphysical degree of freedom to the theory. The pathological-free theory of massive gravity is proposed by de Rham, Gabadadze, and Tolley (dRGT) [57, 58]. In dRGT massive gravity, graviton mass term is described in term of non-linear Stueckelberg fields. The Stueckelberg fields are not fundamental but rather auxiliary fields to help preserve diffeomorphism invariance in massive gravity theory. By treating massive gravity as a small correction to GR, diffeomorphism invariance remains intact at the first order perturbation. Remarkably, the correction term can be introduced as coupling between the perturbation and background Stueckelberg field [59]. This effectively renders a mass term for the graviton. In the same manner as the massive graviton, to restore $U(1)$ gauge invariance in the case of dual vector of massive three-form fields, we introduce a scalar Stückelberg field π via

$$B^\mu \rightarrow B^\mu + \partial^\mu \pi. \quad (45)$$

The action reads

$$S = \int d^4x \sqrt{-g} \left(\frac{1}{2\kappa^2} R + \frac{1}{2} (\nabla_\mu (B^\mu + \partial^\mu \pi))^2 - \frac{1}{2} m_A^2 (B^\mu + \partial^\mu \pi)^2 \right), \quad (46)$$

where the action is now invariant under the gauge transformation

$$B^\mu \rightarrow B^\mu + \partial^\mu \chi, \quad \pi \rightarrow \pi - \chi, \quad (47)$$

where the scalar function, $\chi = \chi(x^\mu)$ is an arbitrary function. The action shows the Stueckelberg scalar π couples directly to the vector field via the gauge invariant mass term $B^\mu \partial_\mu \pi$ and $(\partial\pi)^2$. This is exactly analogous to the coupling between the scalar Stueckelberg field ϕ^a and the metric tensor in massive gravity.

To determine the solution of the Stueckelberg field, π , one can evaluate from the the EOM of π , and it reads,

$$\nabla_\mu (B^\mu + \partial^\mu \pi) = 0, \quad (48)$$

where the components of term $(B^\mu + \partial^\mu \pi)$ can be expressed as

$$B^\mu + \partial^\mu \pi = (\partial^t \pi, \zeta(r) + \partial^r \pi, 0, 0). \quad (49)$$

Considering the π field in the static limit, we obtain

$$\nabla_\mu (B^\mu + \partial^\mu \pi) = \frac{1}{r^2} \partial_r (r^2 f(r) [\zeta(r) + \partial_r \pi]).$$

From the EOM of π , one finds

$$\partial_r (r^2 f(r) [\zeta(r) + \partial_r \pi(r)]) = 0. \quad (50)$$

The derivative of $\pi(r)$ with respect to r , $\partial_r \pi(r) \equiv \pi'(r)$ can be expressed as

$$\pi'(r) = \frac{c_0}{r^2 f(r)} - \zeta(r), \quad (51)$$

where c_0 is the integration constant. The component $\partial_r \pi(r)$ is important for modifying the axial perturbation potential. The mass term contributes to the energy-momentum tensor, which is given by

$$T_{\mu\nu}^{(m)} = m_A^2 (B_\mu + \partial_\mu \pi) (B_\nu + \partial_\nu \pi) - \frac{1}{2} m_A^2 g_{\mu\nu} (B^\alpha + \partial^\alpha \pi)^2. \quad (52)$$

This modifies the EFE, and therefore, backreacts on the potential governing metric perturbations. The modified effective potential ΔV for tensor perturbations can be defined by the following expression

$$\Delta V(r) = \delta T_{\mu\nu}^{(m)}. \quad (53)$$

According to Stueckelberg's mechanism, we defined a new field variable \mathcal{A}^μ as

$$\mathcal{A}^\mu \equiv B^\mu + \partial^\mu \pi, \quad (54)$$

then, $T_{\mu\nu}^{(m)}$ can be rewritten as

$$T_{\mu\nu}^{(m)} = m_A^2 \mathcal{A}_\mu \mathcal{A}_\nu - \frac{1}{2} m_A^2 g_{\mu\nu} \mathcal{A}_\alpha \mathcal{A}^\alpha \quad (55)$$

The modified potential that projected onto gravitational perturbation is given by.

$$\Delta V \sim m_A^2 \mathcal{A}_\mu \mathcal{A}^\mu. \quad (56)$$

Noting that inclusion of the mass term of the three-form fields as the modified potential of the perturbation, we still cannot obtain the double peak structure of the effective potential. In order to produce the second peak as well as to keep the modified potential invariance under the gauge transformation with the Stueckelberg mechanism, it is necessary to introduce additional terms. Accordingly, we propose the following form for the perturbed potential inspired by the Ratra–Peebles potential (inverse power law field) [60, 61]. It reads,

$$\begin{aligned}\Delta V(r) &= m_A^2 \mathcal{A}_\mu \mathcal{A}^\mu + \lambda (\mathcal{A}_\mu \mathcal{A}^\mu)^{-2} \\ &= m_A^2 \frac{c_0^2}{r^4 f(r)^3} + \lambda \left(\frac{c_0^2}{r^4 f(r)^3} \right)^{-2},\end{aligned}\tag{57}$$

where $\mathcal{A}_\mu \mathcal{A}^\mu = \frac{1}{f} (\zeta + \pi')^2$ and λ is a coupling parameter that quantifies the strength of the new interaction term. The term $\lambda (\mathcal{A}_\mu \mathcal{A}^\mu)^{-2}$ is crucial to shaping the potential to exhibit a double peak while preserving gauge invariance.

We are particularly aware of the behavior of the effective potential, which asymptotically approaches zero near both the black hole and the cosmological horizons, but diverges at the horizons themselves. To maintain consistency with the condition of asymptotic flatness, we restrict our analysis to regions sufficiently close to, but not exactly at, the black hole and cosmological horizons.

2. Calculation of time-domain wavefunction

We use the light cone coordinate, where $u = t - r_*$ is the retarded time and $v = t + r_*$ is the advanced time. In terms of the light cone coordinate u and v , the wave equation (41) becomes [62]

$$4 \frac{\partial^2 \Psi}{\partial u \partial v} + V_{\text{eff}}(u, v) \Psi = 0,\tag{58}$$

where $V_{\text{eff}} = V_{\text{GP}}$ in the case of massless three-form fields, and $V_{\text{eff}} = V_{\text{GP}} + \Delta V$ for the inclusion of the modified potential case. To evaluate the wavefunction $\Psi(t, r_*)$, we use the following discretization scheme [62]. The coordinates u and v increases by discrete step Δ . In the discrete domain, the differential equation is defined by

$$\Psi(N) = \Psi(W) + \Psi(E) - \Psi(S) - \frac{\Delta^2}{8} V_{\text{eff}}(S) \left[\Psi(W) + \Psi(E) \right],\tag{59}$$

where the points N , S , E , and W refer to points on a compass on a null rectangle. These points are defined as $N : (u + h, v + h)$, $W : (u + h, v)$, $E : (u, v + h)$ and $S : (u, v)$.

B. Frequency-domain : QNMs of black hole

A linear perturbation on black hole results in an oscillation which can be described by QNMs [63]. A characteristic oscillation signal with corresponding complex frequencies which depend on black hole parameters.

Black hole perturbation equation is often put into the Schrödinger-like equation with effective potential 41. This equation can be written in the Regge-Wheeler equation which solely radial-dependence. By using, the ansatz

$$\Psi(t, r_*) = e^{-i\omega t} \psi(r_*), \quad (60)$$

Eq. (41) becomes

$$\frac{d^2\psi}{dr_*^2} + \left[\omega^2 - V_{\text{eff}}(r) \right] \psi = 0, \quad (61)$$

where ω is denoted as the quasinormal frequency [64–70]. Boundary condition associated with quasinormal modes of black hole are

$$\text{Ingoing} \quad : \quad \psi(r_*) \sim e^{-i\omega r_*}, r_* \rightarrow -\infty, \quad (62)$$

$$\text{Outgoing} \quad : \quad \psi(r_*) \sim e^{i\omega r_*}, r_* \rightarrow \infty. \quad (63)$$

At event horizon, only ingoing wave is allowed while only outgoing wave is permitted at asymptotic infinity. This particular boundary condition yields discrete complex frequency $\omega = \omega_R \pm i\omega_I$. The real part describes an oscillation of a perturbed field while imaginary part determining whether it exhibits decaying or growing behavior.

There are several methods to determine quasinormal frequencies, for instance, Asymptotic Iteration Method (AIM) [71, 72], the Continued Fraction Method (CFM) [73], Chebyshev pseudospectral method [74, 75], etc. While the mentioned methods rely on sophisticated numerical scheme, one of the most commonly used is the Wentzel–Kramers–Brillouin (WKB) method. It is regarded as a semi-analytical method and relatively simpler comparing with the other approaches. A huge number of QNMs studies utilise the advantage of WKB method [17, 44, 76–87].

The WKB method has an advantage when an exact form of effective potential is known. The quasinormal frequencies can be directly computed from the effective potential. More importantly, the WKB approach is valid only for potentials with a single-peak structure,

where the wave behavior near the maximum dominates the scattering process. In this work, double-peak potentials are also considered due to the presence of ΔV . Therefore, the WKB method might not be suitable here. To obtain the quasinormal frequencies, we extract frequencies profile from the time-domain profile of QNMs via the Prony method instead [19, 29, 88–90].

Thus, for a massless case, we will determine quasinormal frequencies of gravitational perturbation around three-form fields black hole via the 6th-order WKB and the Prony method. When three-form fields acquire mass via the Stueckelberg mechanism, the frequencies are obtained from the Prony method.

1. WKB method

The 1st-order WKB method is firstly introduced by Schutz and Will [76] and later is extended with higher order correction terms [77, 78, 82]. The WKB method is based on the problem of waves scattering near the peak of the potential barrier $V(r_*)$ in quantum mechanics, where ω^2 acts as energy. In this work, we consider the 6th-order WKB. In order to obtain the QNMs, we rewrite (61) as

$$\frac{d^2\psi}{dr_*^2} + Q(r_*)\psi(r_*) = 0. \quad (64)$$

where $Q \equiv \omega^2 - V(r_*)$. The quasinormal frequencies can be found by solving the following formula [78]

$$\frac{iQ_0}{\sqrt{2Q_0''}} - \bar{\Lambda}_2 - \bar{\Lambda}_3 - \bar{\Lambda}_4 - \bar{\Lambda}_5 - \bar{\Lambda}_6 = n + \frac{1}{2}. \quad (65)$$

$Q_0 = \omega^2 - V_0$ and V_0 is the value of the potential at the maximum point. We denote second derivative with respect to tortoise coordinate i.e., $Q_0'' = d^2Q/dr_*^2|_{r=r_{max}}$. An overtone number is denoted by integer n . The correction terms $\bar{\Lambda}_{2-6}$ up to 6th-order can be found in [77, 78]. When the effective potential V is independent of ω , the quasinormal frequencies are obtained as

$$\omega = \sqrt{-i \left[\left(n + \frac{1}{2} \right) + \sum_{k=2}^6 \bar{\Lambda}_k \right] \sqrt{-2V_0''} + V_0}. \quad (66)$$

We will employ this formula in the following analysis to obtain the quasinormal frequencies of the massless three-form black hole only.

2. Prony method

To evaluate the QNMs during the ringdown phase, we fit the time-domain profile by treating it as a sum of damped exponentials

$$\Psi(t) \simeq \sum_{n=1}^p C_n e^{-i\omega_n t}. \quad (67)$$

However, the calculation is complicated. In 1795, Prony proposes a generalized approach for fitting a sum of damped exponentials, known as the Prony method [91]. We assume that the ringdown phase begins at $t_0 = 0$ and ends at $t = Nh$, where $N \geq 2p - 1$. Here, h is the fixed time interval between consecutive samples of the signal $\Psi(t)$, set by the data acquisition rate. Then, the relation (67) is satisfied for each point m of the time-domain profile as

$$x_m = \Psi(mh) = \sum_{n=1}^p C_n e^{-i\omega_n mh} \equiv \sum_{n=1}^p C_n z_n^m. \quad (68)$$

We use Prony method to determine z_n from the data x_m . Then, we calculate QNFs (ω_n) from z_n . To find z_n , we define a polynomial $\tilde{A}(z)$ as follows

$$\tilde{A}(z) = \prod_{n=1}^p (z - z_n) = \prod_{k=0}^p \alpha_k z^{p-k}, \quad \alpha_0 = 1, \quad (69)$$

and consider the summation

$$\sum_{k=0}^p \alpha_k x_{m-k} = \sum_{k=0}^p \alpha_k \sum_{n=1}^p C_n z_n^{m-k} = \sum_{n=1}^p C_n z_n^{m-p} \sum_{k=0}^p \alpha_k z_n^{p-k}. \quad (70)$$

Then, we obtain

$$\sum_{k=1}^p \alpha_k x_{m-k} = -x_m. \quad (71)$$

Using $m = p, \dots, N$ in (72), we obtain $N - P + 1 \geq p$ linear equation for α_k , which can be expressed in matrix form as

$$X\alpha = -x, \quad (72)$$

where

$$X = \begin{pmatrix} x_{p-1} & x_{p-2} & \dots & x_0 \\ x_p & x_{p-1} & \dots & x_1 \\ \vdots & \vdots & \ddots & \vdots \\ x_{N-1} & x_{N-2} & \dots & x_{N-p} \end{pmatrix}, \quad \alpha = \begin{pmatrix} \alpha_1 \\ \alpha_2 \\ \vdots \\ \alpha_p \end{pmatrix}, \quad x = \begin{pmatrix} x_p \\ x_{p+1} \\ \vdots \\ x_N \end{pmatrix}. \quad (73)$$

From the above equation, we can solve for the coefficient matrix α using the expression below

$$\alpha = -(X^\dagger X)^{-1} X^\dagger \mathbf{x}, \quad (74)$$

where X^\dagger is the Hermitian transpose of X . Substituting α into (69), we obtain the roots z_n of the polynomial $\tilde{A}(z)$. Finally, the QNMs can be calculated using the relation below

$$\omega_n = \frac{i}{h} \ln(z_n), \quad (75)$$

with ω_n determined from Eq. (75). The QNMs are fully characterized, completing the Prony method reconstruction of the ringdown signal as a sum of damped exponentials Eq. (67).

V. NUMERICAL RESULTS

In this section, we investigate the behavior of the effective potential (V_{eff}), including the gravitational perturbation potential (V_{GP}) and the potential from the Stueckelberg field (ΔV). Without ΔV , the effective potential of gravitational perturbation is single-peak type. By introducing the modified potential produced by the stueckelberg field, the effective potential becomes double-peak type. Moreover, the inclusion of the stueckelberg field also introduces the mass term of the three-form fields. Exploring the behavior of the potential allows us to analyze and calculate the time-domain profile of the QNMs. In order to numerically solve Eq. (58), we consider the Gaussian profile as the initial data

$$\Psi(0, v) = \exp\left(-\frac{(v - v_c)^2}{2\sigma^2}\right) \quad \text{and} \quad \Psi(u, 0) = 0, \quad (76)$$

where the Gaussian profile is centered at $v_c = 10$ and has a width $\sigma = 3$. The initial position of the Gaussian profile, v_c , is placed near the peak of V_{GP} . Here, we particularly focus on the fundamental mode ($n = 0$) and spherical harmonics with $l = 2$ due to their crucial contribution to the ringdown gravitational waves following the merger of binary black holes [92, 93]. The time-domain results are divided into two parts i.e., for single-peak potential and for double-peak potential.

A. Behavior of the single-peak potential

We present the results for the case in which the three-form fields are treated as a massless field. The effective potential from (58) includes only the gravitational perturbation potential,

which can be written as $V_{\text{eff}} = V_{GP}$. As shown in Fig. 2, on the left panel, we illustrate the effective potential V_{GP} as a function of tortoise coordinate for various value of a_1 . The potential exhibits a single peak structure for several values of a_1 . It is observed that at $a_1 = 0.0046875$, the effective potential is closely similar to the effective potential for the gravitational perturbation of a Sch-BH.

We also determine the time-domain wave function resulting from the effective potential by integrating (58) using the finite difference method (59) and employing (76) as the initial data. As shown in the right panel of Fig. 2, the time-domain profile at $a_1 = 0.0046875$ resembles to the time-domain profile of a Sch-BH. As a_1 increases, the time-domain wave function demonstrates a decreasing amplitude and a slower rate of decay. We observe that the time-domain wave function at $a_1 = 0.3$ decays significantly slower than at other values of a_1 .

We have evaluated the QNMs to examine how a_1 affects both the oscillation frequency and the rate of decay by using the 6th-order WKB and the Prony method as shown in Table I. At small a_1 , the real part of frequencies are closely match between the two methods. As a_1 increases, the difference in real part becomes more evident. We also find that, the real and imaginary part of quasinormal frequencies decrease (in magnitude for ω_i) with increasing a_1 . This means the time-domain wave function oscillates more slowly as a_1 increases and similar to the the decay rate. From these results, we find that in the case of a single-peak potential, the effective cosmological constant affects the oscillation of the time-domain wave function. An increasing in the effective cosmological constant results in slower oscillations and decay rate of the time-domain waveform. This is consistent with the results found in [49].

B. Behavior of the double-peak potentials

In the previous case, we examine how a_1 affects the effective potential. In this case, we explore the effect of the mass of the three-form fields (m_A), the coupling parameter λ and constant c_0 on the effective potential, as introduced in section IV A 1. As shown in Fig. 3 on the upper panel, the effective potential in this case has a double-peak structure. We categorize our results into three cases based on the distance between the two peaks, from close to large, each corresponding to specific values of a_1 , namely 0.15, 0.009375, and

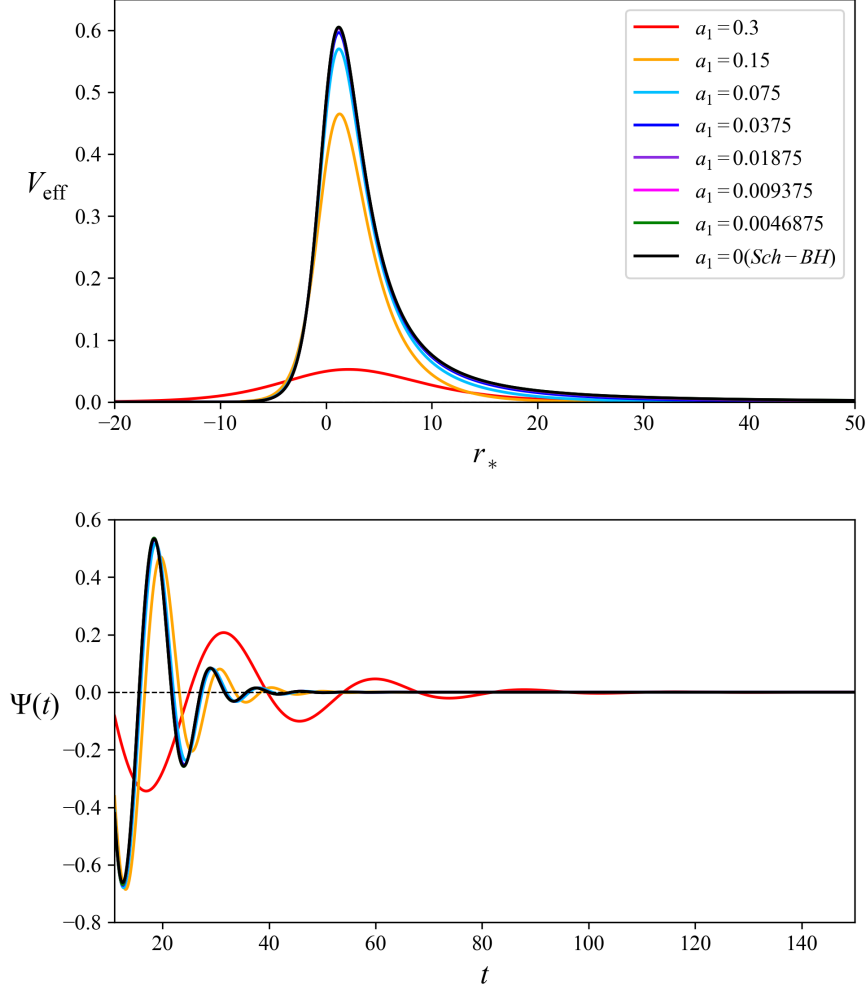


FIG. 2: The upper figure shows the $l = 2$ effective potentials for gravitational perturbations of the three-form black hole, without the modified potential, as a function of the tortoise coordinate r_* . The lower figure shows the time-domain waveform for gravitational perturbation of the three-form black hole, as observed at $r_* = 10$. The plots are presented for varying values of a_1 .

0.0046875.

1. $a_1 = 0.15$

In this case, the modified potential leading to the right peak while the left peak constitutes from the gravitational perturbation potential as can be seen from the top panel of Fig. 3. We remark that, in this case, we set ratio $m/\lambda \sim 10^1$ for all values of c_0 . The two potentials

a_1	6th-order WKB	Prony
0.3	0.198983 - 0.063607 <i>i</i>	0.222702 - 0.058726 <i>i</i>
0.15	0.656713 - 0.159179 <i>i</i>	0.655283 - 0.157871 <i>i</i>
0.075	0.725699 - 0.173452 <i>i</i>	0.726174 - 0.170632 <i>i</i>
0.0375	0.741915 - 0.176717 <i>i</i>	0.741589 - 0.174282 <i>i</i>
0.01875	0.745911 - 0.177517 <i>i</i>	0.745906 - 0.174640 <i>i</i>
0.009375	0.746907 - 0.177716 <i>i</i>	0.746901 - 0.174838 <i>i</i>
0.0046875	0.747156 - 0.177765 <i>i</i>	0.747150 - 0.174887 <i>i</i>
0(Sch-BH)	0.747239 - 0.177782 <i>i</i>	0.747237 - 0.177564 <i>i</i>

TABLE I: The fundamental QNMs ($n = 0$) for gravitational perturbations of the three-form black hole in the single-peak potential case with $M = 1/2$ and $l = 2$ for various values of a_1 . The quasinormal frequencies are calculated using the 6th-order WKB method and the Prony method.

are almost inseparable. Moreover, it is evident that the value of c_0 clearly influences the amplitude of both potentials. As illustrated in Fig. 3 on the bottom panel, the waveforms corresponding to each c_0 display distinct amplitudes and decay rates at late time. Their behavior is determined by the pattern of the effective potential. The waveform has the largest amplitude and fastest decay at $c_0 = 0.90$ (red line). At this value of c_0 , the amplitude of the modified potential is larger than the amplitude of the gravitational potential. We observe that the waveform has the smallest amplitude and slowest decay at $c_0 = 0.70$ (blue-dotted line), where the amplitude of the interaction potential is lower than the amplitude of the gravitational perturbation potential. At $c_0 = 0.77$ (black-dashed line), we notice that the amplitude of the interaction potential is nearly equal to the amplitude of the gravitational perturbation potential. The waveform for this c_0 is represented by the black line in Fig. 3 on the bottom panel. We compute the corresponding frequency using the Prony method listed in Table II.

In summary, from the above results, when the black hole horizon and cosmological horizon are relatively close, it is found that c_0 is directly proportional to the amplitude of the waveform but not to the decay rate.

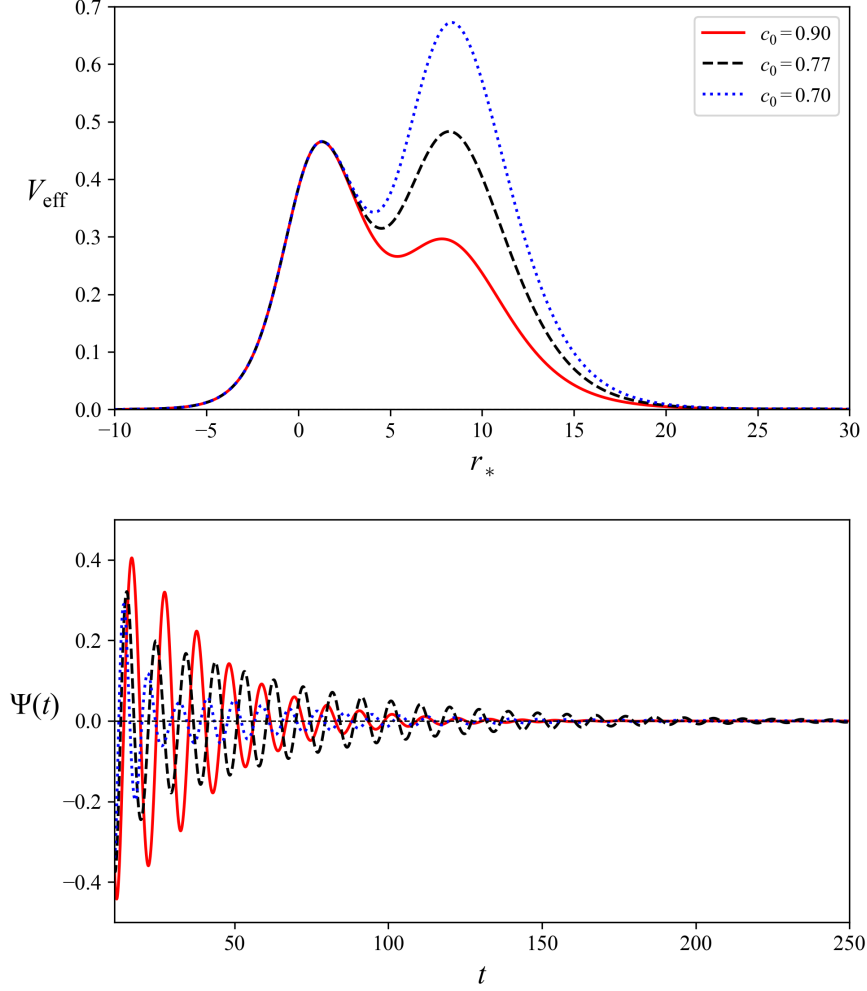


FIG. 3: The (upper) $l = 2$ effective potentials with modified term and the (lower) time-domain waveform for gravitational perturbations of the three-form black hole with $M = 1/2$ and $a_1 = 0.15$, as observed at $r_* = 10$. The modified potential occurs on the right hand side. In this case, we vary three values of c_0 : the red line represents $c_0 = 0.90$, the black-dashed line represents $c_0 = 0.77$, and the blue-dotted line represents $c_0 = 0.70$. The ratio of $m_A/\lambda \sim 10^1$

2. $a_1 = 0.009375$

From the top panel of Fig. 4, we observe that the modified potential appears as the right peak. Notably, the modified potential has a larger width than the gravitational perturbation potential. We vary the parameter c_0 to values 57, 50 and 45, represented by the red, black-dashed, and blue-dotted lines, respectively. Here, we fix the ratio m/λ to $\sim 10^3$. As

expected, only the modified potentials are affected by the mass of the three-form fields.

In the bottom panel, we illustrate the waveform for various value of c_0 . At early time, the waveform exhibits behavior similar to that observed in the single-peak case. At late time, however, distinctive waveforms emerge which is a consequence of the difference in value of c_0 . For all value of c_0 , we notice that the late time wave forms develop nearly at the same time with different amplitudes. The phase and amplitude are influenced by the amplitude of the modified potential.

In this case, we find that the amplitudes of both the modified potential and the reconstructed waveforms are proportional to c_0 . The associated quasinormal frequencies for GWs echoes in this case are shown in Table II. We observe that as c_0 increases, the real part of ω also increases where the decay rate decreases with c_0 .

3. $a_1 = 0.0046875$

In this case, similar to the case of $a_1 = 0.009375$, the modified potential appears on the right side of the gravitational perturbation potential. Here, we have used $m_A/\lambda \sim 10^4$ with parameters $c_0 = 100, 110$ and 120 . These values affect on the amplitude of the effective potential, with a noticeable impact on the modified potential. The higher the c_0 , the smaller the amplitude of the modified potential. The time-domain profiles are shown at the bottom panel of Fig. 5. At early times, it is found that c_0 has a minimal effect on the amplitude and phase of the waveforms. At late times, c_0 impacts the occurrence timing of the reconstructed waveforms.

We observe that at $c_0 = 100, 110$ and 120 , the reconstructed signal reaches its peak the at about $t = 300, 330$ and 380 , respectively. In addition, second echoes signal can be seen for $c_0 = 100, 110$ at $t = 350, 400$ where $c_0 = 120$ develops such signal at later time (not display in the plot). According to these results, we observe that the value of c_0 does not influence the amplitude of the reconstructed waveforms.

In summary, we find that the time required for the reconstructed waveforms to occur is inversely proportional to the mass of the three-form fields. The associated quasinormal frequencies for the double-peak structure are calculated using the Prony method. The results for have been provided in Table II.

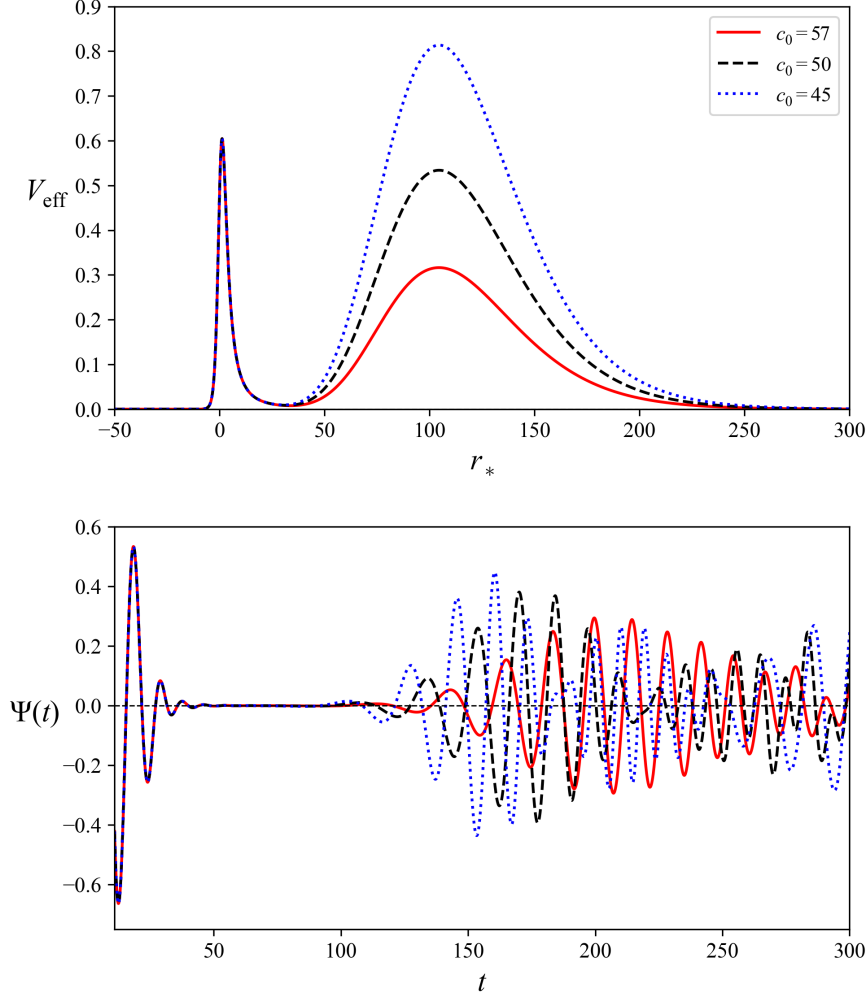


FIG. 4: The (upper) $l = 2$ effective potentials with interaction term and the (lower) time-domain profiles for gravitational perturbations of the three-form black hole with $M = 1/2$ and $a_1 = 0.009375$, as observed at $r_* = 10$. The modified potential occurs on the right hand side. In this case, we vary three values of c_0 : the red line represents $c_0 = 57$, the black-dashed line represents $c_0 = 50$, and the blue-dotted line represents $c_0 = 45$. The ratio of $m_A/\lambda \sim 10^3$.

VI. CONCLUSION

In the present work, the gravitational perturbation of the massless three-form black hole is investigated. Static spherically symmetric black hole in Sch-dS-like form is obtained. The presence of three-form fields effectively manifests itself as a cosmological constant. The time evolution of GWs is analyzed through gravitational perturbation by using discretization

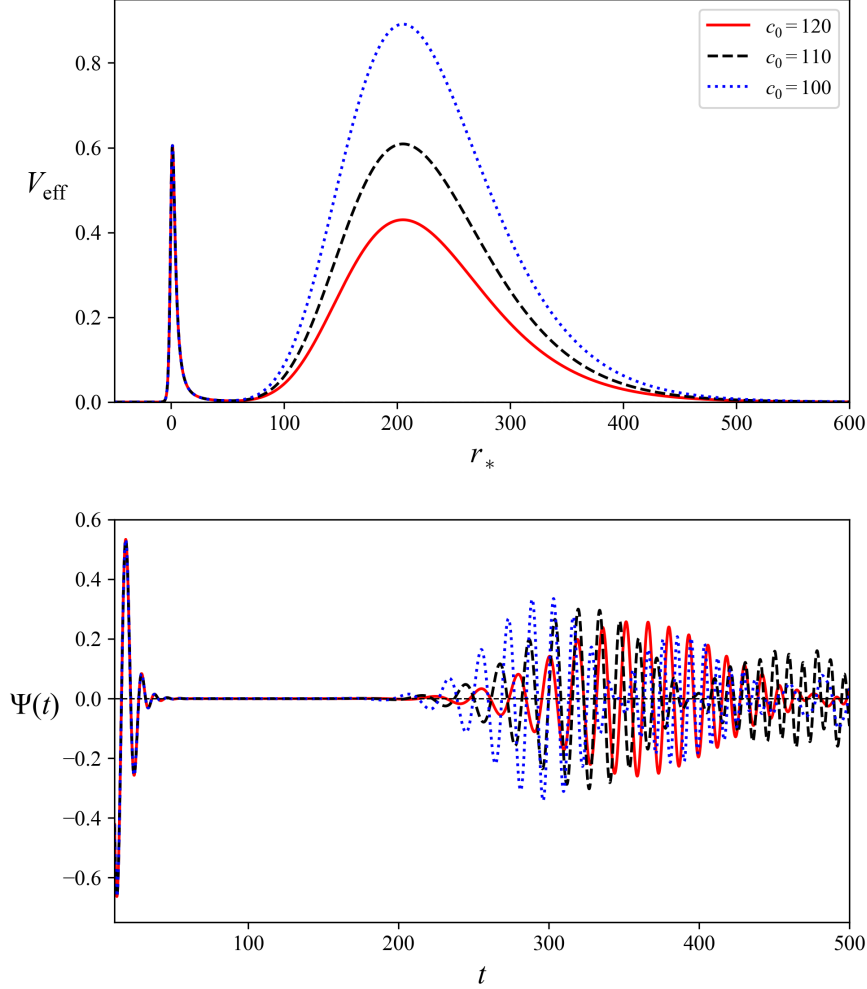


FIG. 5: The (upper) $l = 2$ effective potentials with interaction term and the (lower) time-domain waveform for gravitational perturbations of the three-form black hole with $M = 1/2$ and $a_1 = 0.0046875$. The modified potential occurs on the right hand side. In this case, we vary three values of c_0 : the red line represents $c_0 = 120$, the black-dashed line represents $c_0 = 110$, and the blue-dotted line represents $c_0 = 100$. The ratio of $m_A/\lambda \sim 10^4$.

scheme. For the massless three-form fields, the gravitational perturbation potential exhibits a single-peak structure. In this case, we find that the effective cosmological constant strongly affects both the amplitude and decay rate of the time-domain waveform. In addition, we observe no echo signal. When the effective cosmological constant approaches zero, we find similar waveform as of the Sch-BH.

More importantly, the massive case of the three-form fields are also examined, with a Stueckelberg field introduced to restore gauge invariance. The equation of motion for the

$a_1 = 0.3, m_A/\lambda = 10^1$			
c_0	0.70	0.77	0.90
ω	0.699059 - 0.023419 <i>i</i>	0.658883 - 0.018819 <i>i</i>	0.393392 - 0.032323 <i>i</i>
$a_1 = 0.0375, m_A/\lambda = 10^3$			
c_0	45	50	57
ω	0.475379 - 0.076450 <i>i</i>	0.481184 - 0.029184 <i>i</i>	0.488927 - 0.008711 <i>i</i>
$a_1 = 0.0046875, m_A/\lambda = 10^4$			
c_0	100	110	120
ω	0.491081 - 0.028172 <i>i</i>	0.492917 - 0.004245 <i>i</i>	0.493871 - 0.003375 <i>i</i>

TABLE II: The fundamental QNMs ($n = 0$) for gravitational perturbations of the three-form black hole in the double-peak potential case with $M = 1/2$ and $l = 2$. The QNMs in this case examine the results for three values of a_1 , with each value changing the ratio m_A/λ and c_0 . In this scenario, echoes occur due to the modified potential. The QNMs are calculated using the Prony method.

Stueckelberg field leads to a modification of the effective potential, resulting in a double-peak structure. The existence of a double-peak potential produces GWs echoes at late times in the time-domain profile. The echo signals are then analyzed by considering distinct values of a_1 and c_0 . A smaller a_1 results in greater spacing between two peaks, causing the echo signal to develop more slowly than with a larger a_1 . A higher value of parameter c_0 increases the potential's height, which in turn reduces the amplitude of the echo signal.

The ratio of m_A/λ strongly affects the modified potential. To generate a double-peak effective potential, the ratio m_A/λ must be within $10^3 - 10^4$, corresponding to c_0 on the order of $10^1 - 10^2$. The constant c_0 has a significant impact on the characteristics of the echoes. As a result, the behavior of the echoes depends on the distance between the black hole horizon and the cosmological horizon, as well as on the amplitudes of the modified potential. This work shows that gravitational wave echoes emerge when the black hole horizon and cosmological horizon are sufficiently distant, while no echoes are produced in the near-extremal case. The QNMs of the three-form black hole are calculated by using the 6th-order WKB and Prony methods. We find that both methods agree very well. In

addition, as a_1 increases the real part of the frequencies decreases while the imaginary part becomes less negative. From our analysis, we find no evidence of unstable modes. The analysis presented here is relevant to the cosmological no-hair theorem [94]. As a result, this also confirms that the de Sitter background is perturbative stability [95].

Acknowledgments

We thank Yanapat Limrachadawong for valuable discussions and contributions to exploring the methods for presenting the time-domain profiles. Special thanks also go to Nuttaphat Lunrasri for insightful discussions and for ensuring the correctness of the three-form fields analysis. NA is supported by the Research Capability Enhancement Program through a graduate student scholarship from the Faculty of Science, Khon Kaen University, which is gratefully acknowledged. SP and DS are supported by Thailand NSRF via PMU-B [grant number B39G680009]. DS has also received funding support from the Fundamental Fund of Khon Kaen University.

-
- [1] B. P. Abbott, R. Abbott, T. Abbott, M. Abernathy, F. Acernese, K. Ackley, C. Adams, T. Adams, P. Addesso, R. X. Adhikari, et al., Physical review letters **116**, 061102 (2016).
 - [2] Z. Arzoumanian, P. T. Baker, A. Brazier, S. Burke-Spolaor, S. Chamberlin, S. Chatterjee, B. Christy, J. M. Cordes, N. J. Cornish, F. Crawford, et al., The Astrophysical Journal **859**, 47 (2018).
 - [3] T. Regge and J. A. Wheeler, Physical Review **108**, 1063 (1957).
 - [4] F. J. Zerilli, Phys. Rev. D **9**, 860 (1974), URL <https://link.aps.org/doi/10.1103/PhysRevD.9.860>.
 - [5] S. A. Teukolsky, Phys. Rev. Lett. **29**, 1114 (1972), URL <https://link.aps.org/doi/10.1103/PhysRevLett.29.1114>.
 - [6] S. A. Teukolsky, Astrophys. J. **185**, 635 (1973).
 - [7] C. V. Vishveshwara, Nature **227**, 936 (1970).
 - [8] R. A. Konoplya and A. Zhidenko, Rev. Mod. Phys. **83**, 793 (2011), 1102.4014.
 - [9] S. R. Dolan, S. Ponglertsakul, and E. Winstanley, Phys. Rev. D **92**, 124047 (2015), 1507.02156.

- [10] S. Ponglertsakul and E. Winstanley, Phys. Rev. D **94**, 044048 (2016), 1606.04644.
- [11] C. Promsiri, T. Tangphati, E. Hirunsirisawat, and S. Ponglertsakul, Phys. Rev. D **108**, 024015 (2023), 2302.04654.
- [12] K. D. Kokkotas and B. G. Schmidt, Living Rev. Rel. **2**, 2 (1999), gr-qc/9909058.
- [13] S. H. Völkel and K. D. Kokkotas, Class. Quant. Grav. **35**, 105018 (2018), 1802.08525.
- [14] S. Aneesh, S. Bose, and S. Kar, Phys. Rev. D **97**, 124004 (2018), 1803.10204.
- [15] P. Dutta Roy, S. Aneesh, and S. Kar, Eur. Phys. J. C **80**, 850 (2020), 1910.08746.
- [16] M. S. Churilova, R. A. Konoplya, and A. Zhidenko, Phys. Lett. B **802**, 135207 (2020), 1911.05246.
- [17] S. Ponglertsakul, P. Burikham, and S. Pinkanjanarod, Phys. Rev. D **107**, 023020 (2023), 2208.02761.
- [18] H.-P. Nollert, Classical and Quantum Gravity **16**, R159 (1999).
- [19] E. Berti, V. Cardoso, J. A. Gonzalez, and U. Sperhake, Physical Review D—Particles, Fields, Gravitation, and Cosmology **75**, 124017 (2007).
- [20] V. Cardoso, E. Franzin, and P. Pani, Physical review letters **116**, 171101 (2016).
- [21] V. Cardoso and P. Pani, arXiv preprint arXiv:1709.01525 (????).
- [22] V. Ferrari and K. Kokkotas, Physical Review D **62**, 107504 (2000).
- [23] A. Testa and P. Pani, Physical Review D **98**, 044018 (2018).
- [24] H. Liu, P. Liu, Y. Liu, B. Wang, and J.-P. Wu, Physical Review D **103**, 024006 (2021).
- [25] Q. Wang, N. Oshita, and N. Afshordi, Physical Review D **101**, 024031 (2020).
- [26] S. Hui, B. Mu, and P. Wang, Physics of the Dark Universe **43**, 101396 (2024).
- [27] A. Sang, M. Zhang, S.-W. Wei, and J. Jiang, The European Physical Journal C **83**, 291 (2023).
- [28] R. Dong and D. Stojkovic, Physical Review D **103**, 024058 (2021).
- [29] G. Guo, P. Wang, H. Wu, and H. Yang, Journal of High Energy Physics **2022**, 1 (2022).
- [30] P. Dutta Roy, S. Aneesh, and S. Kar, The European Physical Journal C **80**, 850 (2020).
- [31] M.-Y. Ou, M.-Y. Lai, and H. Huang, The European Physical Journal C **82**, 452 (2022).
- [32] W.-L. Qian, Q. Pan, B. Wang, and R.-H. Yue, Physics Letters B **856**, 138874 (2024).
- [33] K. Groh, J. Louis, and J. Sommerfeld, Journal of High Energy Physics **2013**, 1 (2013).
- [34] S. S. Gubser, arXiv preprint hep-th/0010010 (2000).
- [35] T. S. Koivisto and N. J. Nunes, Physics Letters B **685**, 105 (2010).

- [36] T. S. Koivisto and N. J. Nunes, *Physical Review D—Particles, Fields, Gravitation, and Cosmology* **80**, 103509 (2009).
- [37] C. Germani and A. Kehagias, *Journal of Cosmology and Astroparticle Physics* **2009**, 005 (2009).
- [38] A. De Felice, K. Karwan, and P. Wongjun, *Physical Review D—Particles, Fields, Gravitation, and Cosmology* **85**, 123545 (2012).
- [39] K. S. Kumar, J. Marto, N. J. Nunes, and P. V. Moniz, *Journal of Cosmology and Astroparticle Physics* **2014**, 064 (2014).
- [40] S. Chakraborty, S. Mishra, and S. Chakraborty, *The European Physical Journal C* **80**, 1 (2020).
- [41] T. Barreiro, U. Bertello, and N. J. Nunes, *Physics Letters B* **773**, 417 (2017).
- [42] B. J. Barros and F. S. Lobo, *Physical Review D* **98**, 044012 (2018).
- [43] B. J. Barros, B. Dănilă, T. Harko, and F. S. Lobo, *The European Physical Journal C* **80**, 617 (2020).
- [44] T. Tangphati, M. Youk, and S. Ponglertsakul, *Journal of High Energy Astrophysics* **43**, 66 (2024).
- [45] D. Samart, N. Autthisin, and P. Channuie, *Annalen der Physik* **535**, 2300039 (2023).
- [46] A. Dubinsky, *Modern Physics Letters A* **39**, 2450108 (2024).
- [47] S. Fernando and A. Manning, *International Journal of Modern Physics D* **26**, 1750100 (2017).
- [48] P. R. Brady, C. M. Chambers, W. G. Laarakkers, and E. Poisson, *Physical Review D* **60**, 064003 (1999).
- [49] H. Otsuki and T. Futamase, *Progress of theoretical physics* **85**, 771 (1991).
- [50] K. Clough, T. Helfer, H. Witek, and E. Berti, *arXiv preprint arXiv:2204.10868* (2022).
- [51] S. R. Dolan, *Physical Review D* **98**, 104006 (2018).
- [52] W. E. East and F. Pretorius, *Physical review letters* **119**, 041101 (2017).
- [53] M. Fierz and W. Pauli, *Proc. Roy. Soc. Lond. A* **173**, 211 (1939).
- [54] H. van Dam and M. J. G. Veltman, *Nucl. Phys. B* **22**, 397 (1970).
- [55] V. I. Zakharov, *JETP Lett.* **12**, 312 (1970).
- [56] D. G. Boulware and S. Deser, *Phys. Rev. D* **6**, 3368 (1972).
- [57] C. de Rham and G. Gabadadze, *Phys. Rev. D* **82**, 044020 (2010), 1007.0443.
- [58] C. de Rham, G. Gabadadze, and A. J. Tolley, *Phys. Rev. Lett.* **106**, 231101 (2011), 1011.1232.

- [59] R. Dong and D. Stojkovic, Phys. Rev. D **92**, 084045 (2015), 1505.03145.
- [60] P. J. E. Peebles and B. Ratra, Astrophys. J. Lett. **325**, L17 (1988).
- [61] B. Ratra and P. J. E. Peebles, Phys. Rev. D **37**, 3406 (1988).
- [62] C. Gundlach, R. H. Price, and J. Pullin, Physical Review D **49**, 883 (1994).
- [63] S. Chandrasekhar and S. Detweiler, Proceedings of the Royal Society of London. A. Mathematical and Physical Sciences **344**, 441 (1975).
- [64] D. Birmingham, Physical Review D **64**, 064024 (2001).
- [65] H.-c. Kao and D. Tomino, Physical Review D—Particles, Fields, Gravitation, and Cosmology **77**, 127503 (2008).
- [66] R. Dal Bosco Fontana, Classical and Quantum Gravity (2023).
- [67] L.-M. Cao, L.-B. Wu, Y. Zhao, and Y.-S. Zhou, Physical Review D **108**, 124023 (2023).
- [68] X. He, B. Wang, and S. Chen, Physical Review D—Particles, Fields, Gravitation, and Cosmology **79**, 084005 (2009).
- [69] J. Sadeghi, A. Chatrabhuti, and B. Pourhassan, International Journal of Theoretical Physics **50**, 129 (2011).
- [70] S. Musiri and G. Siopsis, Physics Letters B **563**, 102 (2003).
- [71] H. Cho, A. Cornell, J. Doukas, and W. Naylor, Classical and Quantum Gravity **27**, 155004 (2010).
- [72] H. Ciftci, R. L. Hall, and N. Saad, Journal of Physics A: Mathematical and General **36**, 11807 (2003).
- [73] E. W. Leaver, Proceedings of the Royal Society of London. A. Mathematical and Physical Sciences **402**, 285 (1985).
- [74] J. P. Boyd, *Chebyshev and Fourier spectral methods* (Courier Corporation, 2001).
- [75] A. Aragón, R. Bécar, P. González, and Y. Vásquez, Physical Review D **103**, 064006 (2021).
- [76] B. F. Schutz and C. M. Will, The Astrophysical Journal **291**, L33 (1985).
- [77] S. Iyer and C. M. Will, Phys. Rev. D **35**, 3621 (1987), URL <https://link.aps.org/doi/10.1103/PhysRevD.35.3621>.
- [78] R. Konoplya, Physical Review D **68**, 024018 (2003).
- [79] A. Zhidenko, Classical and Quantum Gravity **21**, 273 (2003).
- [80] P. Burikham, S. Ponglertsakul, and L. Tannukij, Phys. Rev. D **96**, 124001 (2017), 1709.02716.
- [81] S. Ponglertsakul, P. Burikham, and L. Tannukij, Eur. Phys. J. C **78**, 584 (2018), 1803.09078.

- [82] J. Matyjasek and M. Telecka, *Physical Review D* **100**, 124006 (2019).
- [83] R. Konoplya, A. Zhidenko, and A. Zinhailo, *Classical and Quantum Gravity* **36**, 155002 (2019).
- [84] E. Santos, J. Fabris, and J. de Freitas Pacheco, arXiv preprint arXiv:1903.04874 (????).
- [85] S. Ponglertsakul and B. Gwak, *Eur. Phys. J. C* **80**, 1023 (2020), 2007.16108.
- [86] D. J. Gogoi, A. Övgün, and M. Koussour, *The European Physical Journal C* **83**, 700 (2023).
- [87] D. J. Gogoi and S. Ponglertsakul, *The European Physical Journal C* **84**, 652 (2024).
- [88] R. Konoplya and A. Zhidenko, *Reviews of Modern Physics* **83**, 793 (2011).
- [89] A. Chowdhury and N. Banerjee, *Physical Review D* **102**, 124051 (2020).
- [90] B. K. Vishvakarma, D. V. Singh, and S. Siwach, *The European Physical Journal Plus* **138**, 536 (2023).
- [91] G. Baron de Prony, *J. l'École Polytech* **1**, 24 (1795).
- [92] M. Giesler, M. Isi, M. A. Scheel, and S. A. Teukolsky, *Physical Review X* **9**, 041060 (2019).
- [93] N. Sago, S. Isoyama, and H. Nakano, *Universe* **7**, 357 (2021).
- [94] G. W. Gibbons and S. W. Hawking, *Physical Review D* **15**, 2738 (1977).
- [95] G. W. Gibbons, S. W. Hawking, and S. T. Siklos, *Very Early Universe* (1983).